FULL-SCALE DYNAMIC TESTS AND ANALYTICAL VERIFICATION OF A FORCE-RESTRICTED TUNED VISCOUS MASS DAMPER

Y. Watanabe
THK Co., Ltd., Tokyo, Japan

K. Ikago & N. Inoue
Tohoku University, Sendai, Japan

H. Kida, S. Nakaminami & H. Tanaka
Aseismic Device, Co., Ltd., Tokyo, Japan

Y. Sugimura & K. Saito
NTT Facilities Inc., Tokyo, Japan

SUMMARY:
The authors have proposed a new seismic control system, the tuned viscous mass damper (TVMD). The basic concept of this device is same as that of a tuned mass damper (TMD). However, unlike a conventional TMD, the proposed device is as small as a conventional oil damper or a buckling restrained brace currently applied to seismic control of a building. Therefore, the device can replace conventional dampers and is expected to obtain better seismic control performance. Furthermore, the optimum design of the TVMD is obtained by using fixed points on its resonance curves.
In this paper, we propose a force-restricted damper mechanism by using rotational friction. Full-scale dynamic tests were conducted using a full-scale force-restricted TVMD having a spring stiffness of 35,500 kN/m, an apparent inertial mass of 5400 t, and force limits of 600 kN and 2000 kN. The test results showed good agreement with the analytical results.

Keywords: Tuned mass damper, Fixed point method, Force restriction, Rotary friction, Flywheel

1. INTRODUCTION

Recently, the authors examined a new seismic control method using a secondary vibration system consisting of a rotational viscous damper equipped with a cylindrical flywheel and a soft spring to connect them to the primary system (Saito, Kurita and Inoue 2007, Saito *et al*. 2008, Kida *et al*. 2010b, Ikago *et al*. 2010a, Ikago *et al*. 2012, Kida *et al*. 2011). The present system is referred to as the tuned viscous mass damper (TVMD). The TVMD realizes a large apparent mass that enables effective seismic control by using a ball screw mechanism. However, a concern with this system is that an excessive response damping force is generated when it is subjected to an excitation in which components resonate according to the secondary system. Kida *et al*. (2011) proposed a method to restrict the reaction force by using a rotary friction mechanism.

In this paper, dynamic tests are conducted on a full-scale force-restricted TVMD (FRTVMD) having a spring stiffness of 35,500 kN/m, an apparent translational mass of 5400 t, and force limits of 600 kN and 2000 kN.

2. TEST SPECIMEN AND ANALYTICAL MODEL

2.1. Outline of the Specimen

Fig. 2.1 shows the loading equipment and full-scale FRTVMD specimen. A sinusoidal excitation or a seismic ground motion record is input through the dynamic actuator, which has a maximum load of

±3000 kN, a maximum amplitude of ±100 mm, and a maximum velocity of ±300 mm/s. Displacements of the cantilever at the base of the specimen, deformations of the rotational viscous damper, and displacements input by the actuator are all measured. The total response force of the damper is measured by a load cell installed at one end of the actuator.

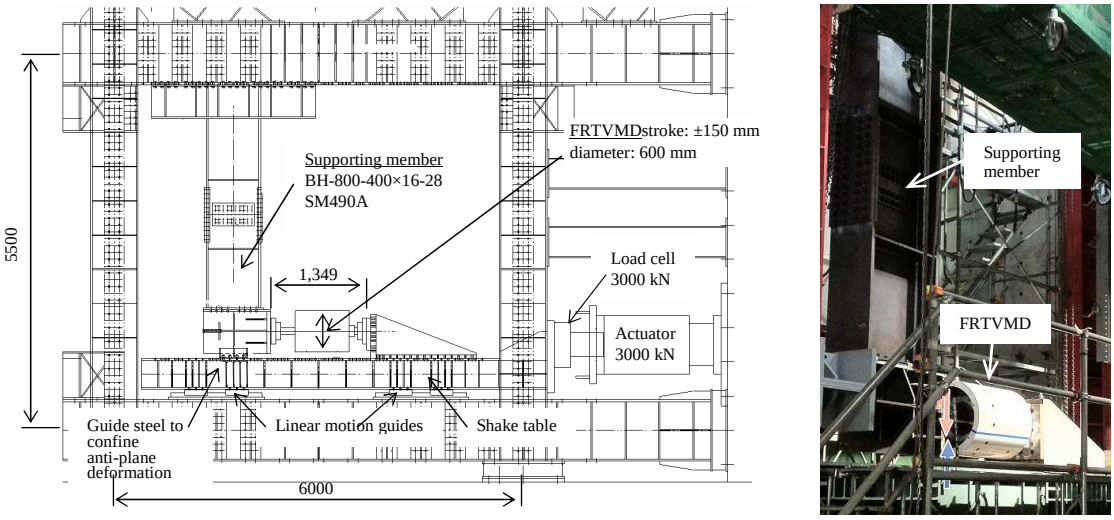

Figure 2.1 Schematic and photograph of full-scale specimen

2.2. Summary of FRTVMD

A schematic of the FRTVMD, which has a cylindrical flywheel and a viscous element enclosed between external and internal tubes, is shown in Fig. 2.2. A large mass moment of inertia resulting from the large-diameter cylindrical flywheel and the high rotational acceleration resulting from the ball screw mechanism generate large inertial torque. This torque is amplified when it is translated back into the translational direction. Thus, the small actual mass of the cylindrical flywheel is amplified several thousand-fold by the ball screw mechanism, and produces a large apparent translational mass. The viscous damping torque generated by the viscous material enclosed between the external and internal tubes is also amplified by the ball screw mechanism to create a large translational damping force.

A rotational frictional material made from ultra-high-molecular-weight polyethylene is inserted between the cylindrical flywheel and the ball screw nut such that the excessive inertial and damping torque is not transmitted to the ball screw. Thus, the response force generated by the damper is restricted to a specified load. The coefficient of friction between the friction material and the ball screw nut is 0.15, and twelve pieces of frictional material are placed on the circumference of the ball screw nut. The limit force is adjusted by changing the axial force applied to the coned disk springs that hold the friction materials.

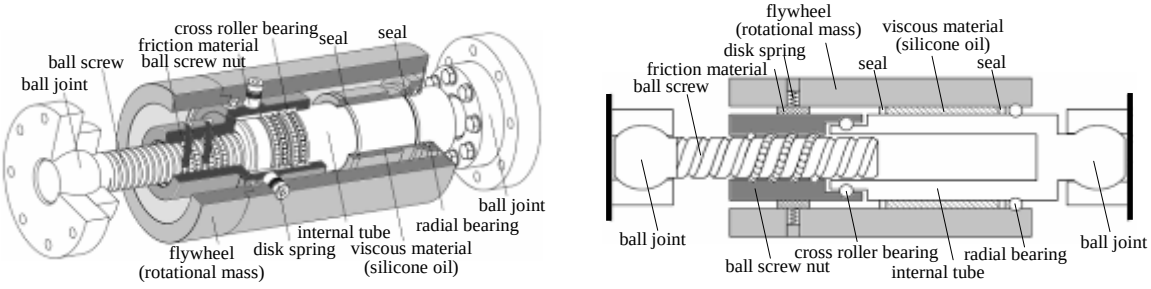

Figure 2.2 Schematic of FRTVMD

A FRTVMD consists of a VMD, whose response force is restricted by the rotary friction (Figs. 2.2 and 2.3(a)), and a supporting member (Fig. 2.3(b)) connected in series. While the traction between the cylindrical flywheel and the ball screw nut continues to be transmitted, the secondary vibration system consisting of the secondary mass and the supporting spring has a fundamental circular frequency of $\omega = \sqrt{k_b / m_i}$, where m_i and k_b are the apparent translational mass and supporting member stiffness, respectively. In the analytical model, the combination of an elastic spring and a friction slider produces an elastic-perfect plastic material.

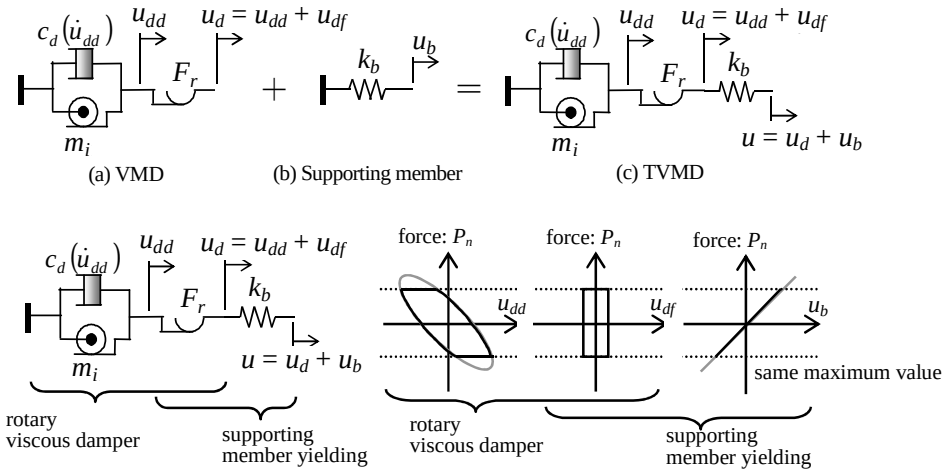

Figure 2.3 Analytical model of TVMD

Hereinafter, u_d and θ represent the axial displacement input to the FRTVMD and the corresponding angular displacement, respectively. θ_f and u_{df} represent the angular slip displacement in the rotary frictional mechanism and the corresponding virtual translational slip displacement, respectively. θ_d and u_{dd} represent the angular displacement of the flywheel and the corresponding translational displacement, respectively. When the friction mechanism is not activated, θ_f and u_{df} remain at 0. The relationship between the actual displacements in the rotational direction and the virtual translational displacement is obtained as follows:

$$u_d = u_{df} + u_{dd}\ , \quad \theta = \theta_f + \theta_d\ , \quad u_d = \frac{L_d}{2\pi}\cdot\theta\ , \quad u_{df} = \frac{L_d}{2\pi}\cdot\theta_f\ , \quad u_{dd} = \frac{L_d}{2\pi}\cdot\theta_d \tag{2.1}$$

where L_d is the lead length of the ball screw.

The translational displacements derived from Eq. (2.1) are virtual, no residual displacement remains, and the end of the damper is restored to its original position after it is unloaded.

From Fig. 2.3, the equations of motion of the FRTVMD when subjected to a forced displacement $u(t)$ ($= u_d + u_b$) are obtained as follows.

When the rotary friction mechanism is not activated:

$$u_{df} = 0\ ,\ u_d = u_{dd}\ ,\ \left| c_v \left|\dot{u}_d\right|^{\alpha-1}\dot{u}_d + m_i\cdot\ddot{u}_d \right| = \left| c_v\cdot\mathrm{sgn}(\dot{u}_d)\left|\dot{u}_d\right|^{\alpha} + m_i\cdot\ddot{u}_d \right| < \left|F_r\right|\ ,$$

$$P_n = c_v\left|\dot{u}_d\right|^{\alpha-1}\dot{u}_d + m_i\cdot\ddot{u}_d = c_v\cdot\mathrm{sgn}(\dot{u}_d)\left|\dot{u}_d\right|^{\alpha} + m_i\cdot\ddot{u}_d = k_b\left(u - u_d\right). \tag{2.2a}$$

When the rotary friction mechanism is activated:

$$u_d = u_{df} + u_{dd}\ ,\ \ c_v\cdot\mathrm{sgn}(\dot{u}_{dd})\left|\dot{u}_{dd}\right|^{\alpha} + m_i\cdot\ddot{u}_{dd} = F_r\ ,$$

$$P_n = F_r = k_b\left(u - u_d\right). \tag{2.2b}$$

Here, α is a constant that expresses the nonlinearity of the viscous coefficient; thus, the equations of motion are linear if α equals 1.

The amplification factors of u_d and u_b with respect to inputted harmonic displacement u are expressed as follows (Kida *et al*. 2010b, 2011):

$$\frac{u_d}{u} = \frac{1}{\sqrt{\left\{1-(p/\omega)^2\right\}^2 + \left\{2h_e(p/\omega)\right\}^2}} \times e^{-i\psi_1}, \tag{2.3}$$

$$\frac{u_b}{u} = \sqrt{\frac{(p/\omega)^4 + \left\{2h_e(p/\omega)\right\}^2}{\left\{1-(p/\omega)^2\right\}^2 + \left\{2h_e(p/\omega)\right\}^2}} \times e^{-i(\psi_1-\psi_2)}, \tag{2.4}$$

where $\psi_1 = \tan^{-1}\dfrac{2h_e(p/\omega)}{1-(p/\omega)^2}$, $\psi_2 = \tan^{-1}\dfrac{2h_e(p/\omega)}{-(p/\omega)^2}$, p is the exciting frequency, and $2h_e = c_v\left|\dot{u}_d\right|^{\alpha-1}/(m_i\omega)$.

2.3. Specifications of FRTVMD Specimen

Table 2.1 lists the specifications of the FRTVMD used in the shaking table tests.

Table 2.1 Specifications of FRTVMD

full length of device	Mm	1349
apparent translational mass	Kg	1110
ball screw radius	Mm	50.0
ball screw lead	Mm	20.0
diameter of cylindrical flywheel	Mm	600

To evaluate the variance in the actual manufactured system, built according to our design, we conducted shake table tests on the FRTVMD specimen. The translational apparent mass, constants c_v and α, and supporting member stiffness k_b are evaluated using sinusoidal excitations. Fig. 2.4(a) shows the relationship between the damping force and input displacement when the rotary friction mechanism is not activated. Fig. 2.4(b) shows the relationship between the viscous damping force and the response velocity in the viscous material. Fig. 2.4(c) shows relationship between the restoring force of the supporting member and its deformation.

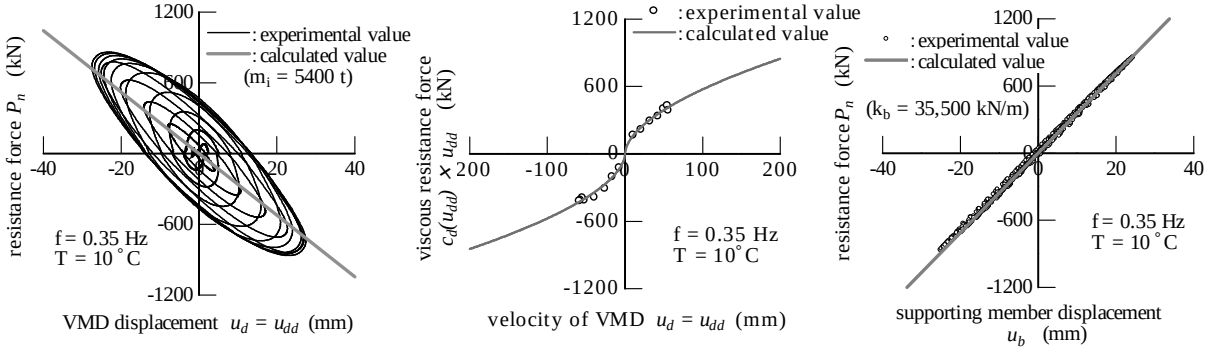

(a) Displacement of VMD and force

(b) Velocity and viscous damping force

(c) Displacement of supporting spring and force

Figure 2.4 Sine wave excitation, frequency 0.35 Hz (with taper wave)

As shown in Fig. 2.4.(a), the hysteresis loop of the viscous mass damper is slanted to the right. This is caused by the apparent mass effect. Let the viscous mass damper displacement $u_d = \delta \sin pt$, then the

resistance force of the damper is $-m_i(p^2\delta)$ at a displacement $u_d = \delta$. Thus, the apparent translational mass of m_i = 5400 t is obtained from the gradient of the gray line in Fig. 2.4(a). Since the actual mass of the flywheel is 0.758 t, the mass amplification factor is about 7124. In Fig. 2.4(b), experimental values, denoted by circles, show the damping forces measured at displacement $u_d = 0$ and acceleration $\ddot{u}_d = 0$ to eliminate the inertial forces. The constants c_v and α are sought such that the curve obtained by Eq. (2.2) fits to the experimental values:

$$c|\dot{u}_d|^{\alpha-1} = 1945 \cdot |\dot{u}_d|^{\alpha-1} \times 1.01^{(15-T)} \text{ (kN·s/m)},$$
$$\alpha = 0.56 \text{ , } 10\ ^\circ\text{C} \leq \text{temperature of viscous fluid } T \leq 20\ ^\circ\text{C}. \quad (2.5)$$

The supporting member stiffness, calculated by the least-squares method from the experimental result shown in Fig. 2.4(c), was k_b = 35,500 kN/m. Thus, the fundamental circular frequency ω of FRTVMD is 2.56 rad/s. We conduct shaking table tests on FRTVMDs with restriction forces of 2000 kN and 600 kN.

3. SHAKING TABLE TESTS USING SINUSOIDAL EXCITATION

In this section, we conduct shaking table tests using sinusoidal excitations to elucidate the frequency response characteristics of the FRTVMD, in order to study the damping effects and confirm the accuracy of the analytical model. The FRTVMD is subjected to the forced sinusoidal displacements of the shaking table. Fig. 3.1 shows the results of the experimental case, in which the limit force is about 2000 kN, the displacement amplitude is 15 mm, and the exciting frequency is 0.35 Hz. In this case, slip displacement in the rotary friction mechanism never occurs. Figs. 3.1 and 3.2 show the amplitude factors and phase angles of the VMD and the supporting spring deformation amplitudes to the input exciting displacement amplitude, respectively.
In Fig. 3.2, experimental results are denoted by solid black circles, and those circled correspond to the case shown in Fig. 3.1. On substituting h_e = 0.2, 0.3, and 0.4 into Eqs. (2.3) and (2.4), we obtain the amplitude factors denoted by the solid, dotted, and dashed lines in Fig. 3.2, respectively. The solid and dashed lines in the hysteresis loops in Fig. 3.1 are the experimental and numerical analysis results, respectively.

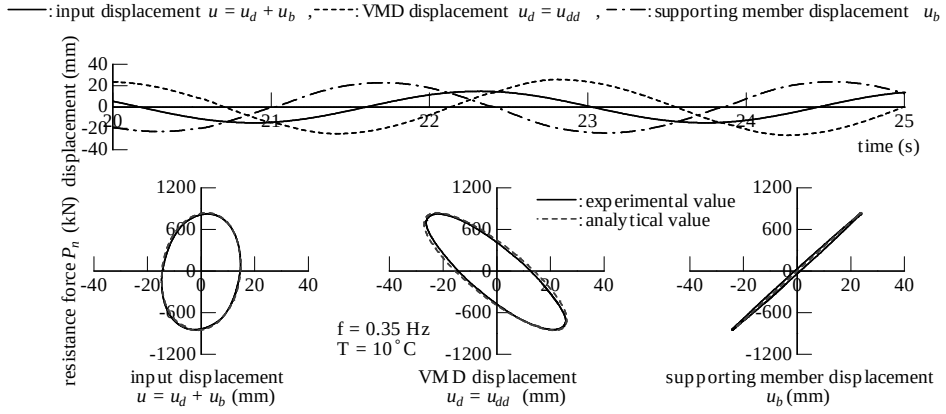

Figure 3.1 Sinusoidal excitation, exciting frequency 0.35 Hz, amplitude 15 mm, restriction force F_r = 2000 kN

From Figs. 3.1 and 3.2, the deformation of the TVMD u_d and that of the supporting member u_b are out of phase by approximately half of a wavelength when the exciting frequency is close to the fundamental circular frequency of the FRTVMD. The response displacements of the TVMD and supporting member are amplified by the secondary vibration system in this case. As a result, the equivalent damping ratio, which is dependent on the nonlinearity of the damping coefficient $c_v|\dot{u}_{dd}|^{\alpha-1}$, decreases as the exciting frequency approaches the fundamental frequency (Fig. 3.2). Although the experimental hysteresis loop of the supporting member shows some hysteretic energy dissipation (Fig.

3.1), the analytical results are in good agreement with the experimental results, and the nonlinear damping coefficient, apparent translational mass, supporting spring stiffness, and restriction force are evaluated accurately.

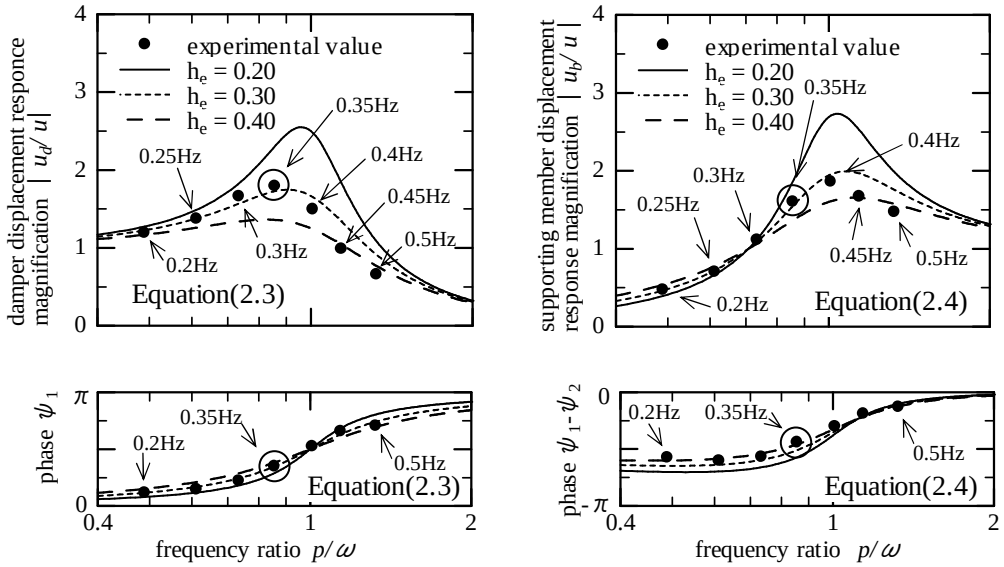

(a) Viscous mass damper: u_d (b) Supporting spring: u_b

Figure 3.2 Displacement response, amplification factor, and phase

Fig. 3.3 shows the experimental results of the forced sinusoidal excitation, in which the exciting frequency is 0.35 Hz, restriction force F_r = 600 kN, and displacement amplitude is 15 mm.

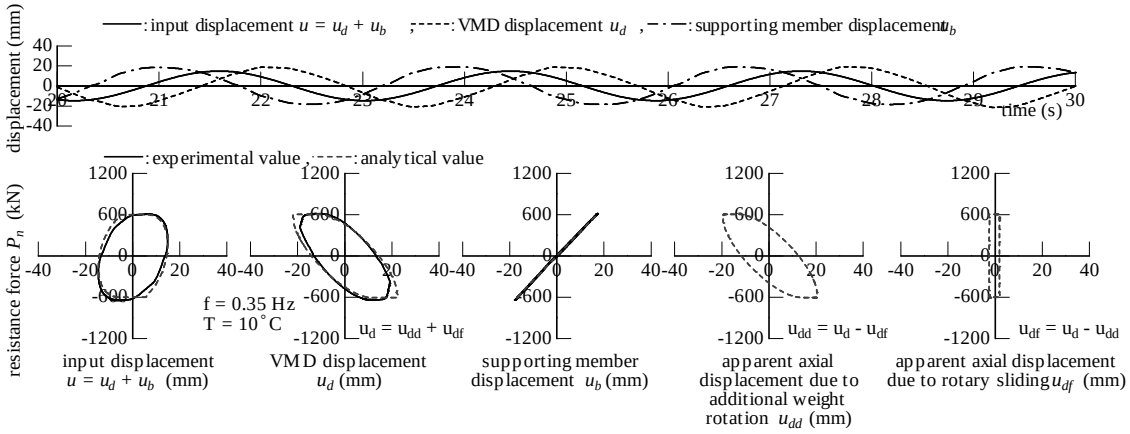

Figure 3.3. Sinusoidal excitation, exciting frequency 0.35 Hz, amplitude 15 mm, restriction force F_r = 600 kN

In this case, slip displacement is observed in Fig. 3.3 because the limit force is low. The analytical results of this case are also in good agreement with the experimental results. The percentage of hysteretic energy dissipated by the friction mechanism is 17.2% of the total energy dissipated by the damper.

4. SHAKING TABLE TESTS USING FLOOR RESPONSES

The FRTVMD used in this experiment is optimally tuned to a structure with a natural period of 2.8 s.

Floor response excitation is obtained from time history analyses when the structure is subjected to the north-south component of the Hachinohe Harbor Office record of the 1968 Tokachi-Oki earthquake.

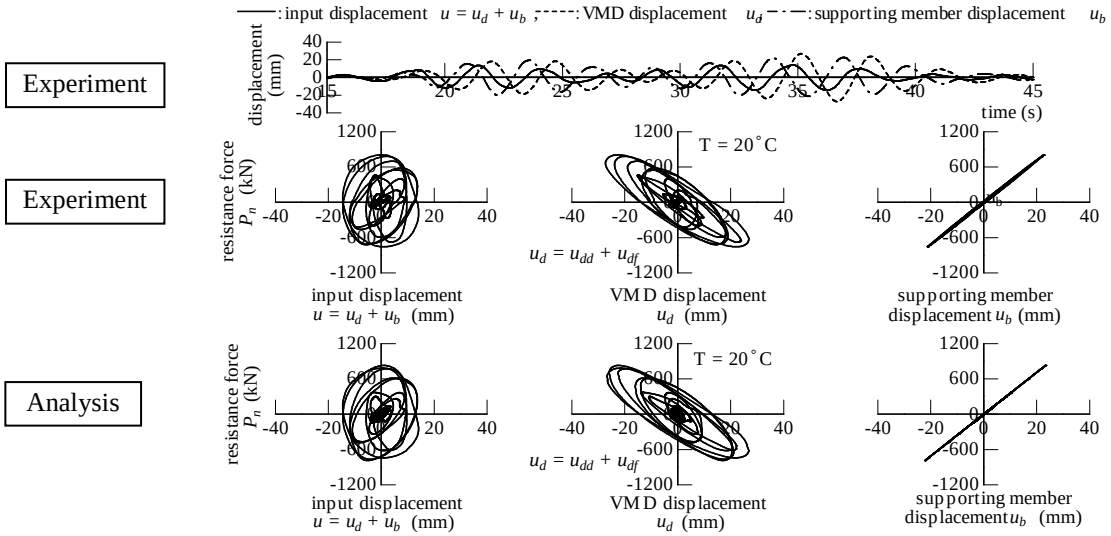

Figure 4.1 Results of experiments and analysis (F_r = 2000 kN; floor response)

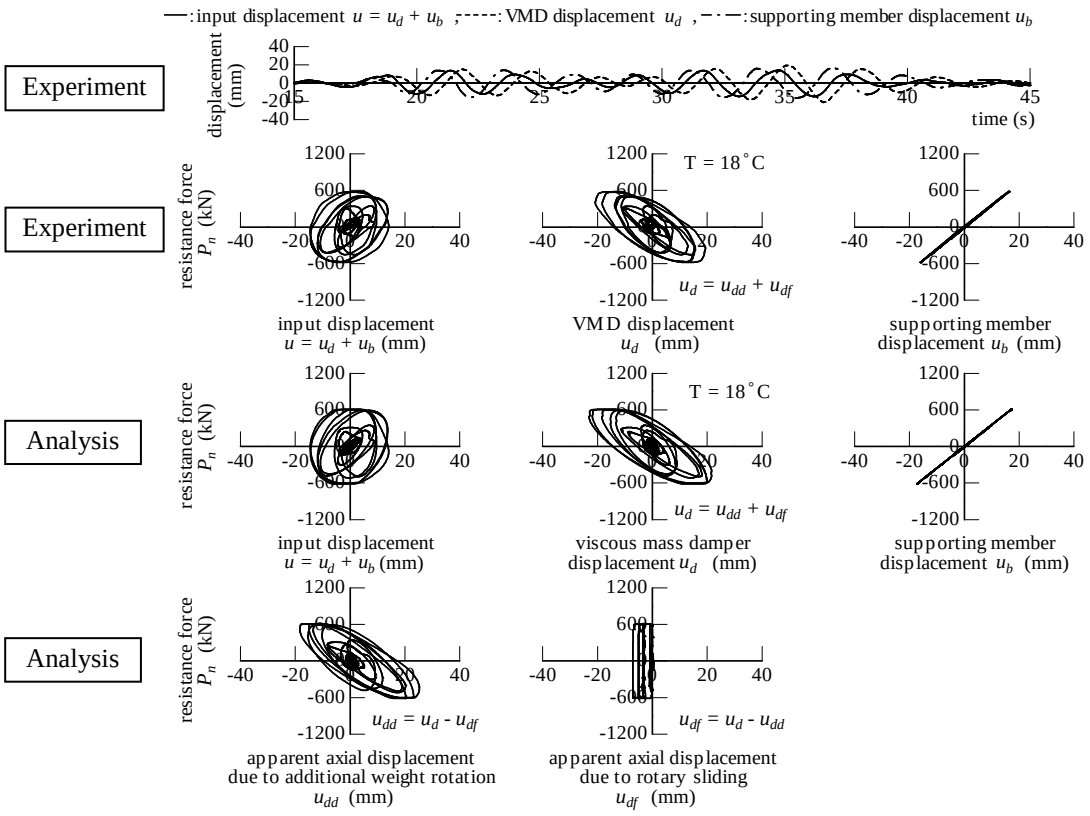

Figure 4.2 Results of experiment and analysis (F_r = 600 kN; floor response)

Fig. 4.1 shows the experimental results, in which the FRVMD with 2000 kN limit force is subjected to the floor response excitation. In this case, slip displacement does not occur in the rotary friction mechanism. The analytical results show good agreement with the experimental results. We observe that the displacements of the VMD and supporting spring are amplified by the secondary vibration system.

Fig. 4.2 shows the experimental results, in which the FRVMD with 600 kN limit force is subjected to the floor response excitation. In this case, slip displacement is observed in the rotary friction mechanism. The analytical results once more show good agreement with the experimental results.

Thus, we have validated our analytical methods for the FRTVMD subjected to a random excitation.

5. CONCLUSIONS

In this paper, we validate our analytical models and methods by applying full-scale shaking table tests to the FRTVMD. The results obtained in this study are as follows:

1) We proposed a method of restricting the reaction force using a rotary friction mechanism in order to limit the excessive response force of the TVMD caused by components resonating at the damping frequency.
2) Our experimental studies verified that the limit force can be controlled by adjusting the axial force applied to the coned disk springs that hold the frictional material.
3) The analytical results showed good agreement with the experimental results, and the apparent translational mass, nonlinear damping coefficient, supporting spring stiffness, and limit force of the damper were evaluated accurately.

REFERENCES

Den Hartog J.P. (1985). Mechanical Vibrations. (4th edn). Dover: New York.

Ikago K., Sugimura Y., Saito K., Inoue N. (2010a). Optimum Seismic Response Control of Multiple Degree of Freedom Structures using Tuned Viscous Mass Dampers. *Proceedings of the Tenth International Conference on Computational Structures Technology*, Valencia, Spain, Paper 164, DOI:10.4203/ccp.93.164.

Ikago K., Saito K., Inoue N. (2012). Seismic control of single-degree-of-freedom structure using tuned viscous mass damper. *Earthquake Engineering and Structural Dynamics*, **Vol.41**, Issue3, 453-474, DOI:10.1002/eqe.1138.

Kaynia A.M., Veneziano D., Biggs J. (1981). Seismic effectiveness of tuned mass dampers. *Journal of Structural Division ASCE* **vol.107(9)**, 1465-1484

Kida H., Nakaminami S., Saito K., Ikago K., Inoue N. (2010b). Verification in Analysis Model of Tuned Viscous Mass Damper Based on Full-Scale Dynamic Tests. *Journal of Structural Construction Engineering Architectural Institute of Japan* **Vol.56B**, 137-146. (in Japanese).

Kida H., Watanabe Y., Nakaminami S., Tanaka H., Sugimura Y., Saito K., Ikago K., Inoue N. (2011). Full-Scale Dynamic Tests of Tuned Viscous Mass Damper with Force Restriction Mechanism and Its Analytical Verification. *Journal of Structural and Construction Engineering Architectural Institute of Japan*, **Vol.76**, No.665, 1271-1280. (in Japanese).

McNamara RJ. (1979). Tuned mass dampers for buildings. *Journal of Structural Engineering ASCE* **vol.103 (9)**, 1785-1798

Saito K., Kurita S., Inoue N. (2007). Optimum response control of 1-DOF system using linear viscous damper with inertial mass and its Kelvin-type modeling. *Journal of Structural Construction Engineering Architectural Institute of Japan* **Vol53B**, 53-66. (in Japanese).

Saito K., Sugimura Y., Nakaminami S., Kida H., Inoue N. (2008). Vibration Tests of 1-Story Response Control System Using Inertial Mass and Optimized Soft Spring and Viscous Element. *Proceedings of the 14th World Conference on Earthquake Engineering*, Beijing, China, Paper ID 12-01-0128.